Recursive T-Matrix Methods for Scattering from Multiple Dielectric and Metallic Objects

Adnan Şahin and Eric L. Miller, *Member, IEEE*

***Abstract*— We present an efficient, stable, recursive T-matrix algorithm to calculate the scattered field from a heterogeneous collection of spatially separated objects. The algorithm is based on the use of higher order multipole expansions than those typically employed in recursive T-matrix techniques. The use of these expansions introduces instability in the recursions developed in [5] and [6], specifically in the case of near-field computations. By modifying the original recursive algorithm to avoid these instabilities, we arrive at a flexible and efficient forward solver appropriate for a variety of scattering calculations. The algorithm can be applied when the objects are dielectric, metallic, or a mixture of both. We verify this method for cases where the scatterers are electrically small (fraction of a wavelength) or relatively large (12λ). While developed for near-field calculation, this approach is applicable for far-field problems as well. Finally, we demonstrate that the computational complexity of this approach compares favorably with comparable recursive algorithms.**

***Index Terms*— Electromagnetic scattering.**

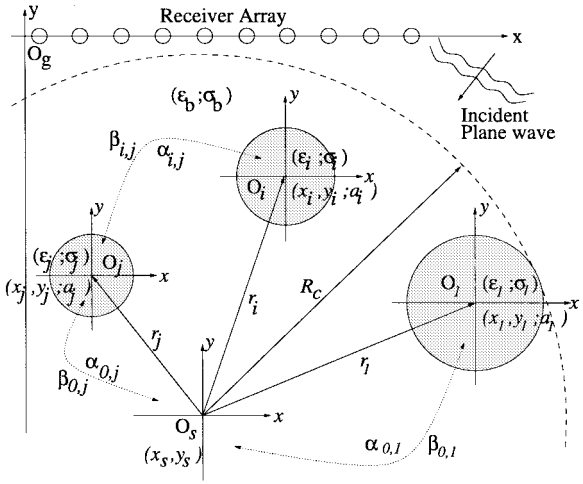

Fig. 1. Near-field geometry and translation matrices.

I. Introduction

CALCULATION of scattered electromagnetic fields is of interest in many application areas. For example, an important component of the solution to many inverse scattering problems is the efficient computation of the scattered fields produced by a collection of scatterers when illuminated by an electromagnetic source. The choice of technique for computing these fields is often driven by a variety of factors, including computational complexity and the flexibility to handle easily a wide range of configurations of scatterers. In practice, the objects of interest can be dielectric, metallic, or mixtures of both. Their sizes can range from subwavelength to a few multiples of a wavelength. Therefore, one desires an efficient flexible forward solver that is useful both for analysis and that can be incorporated into signal processing algorithms.

The most popular forward solver for these and related complex scattering problems—the method of moments (MoM) [1]—is based on a fine discretization of the region of interest and requires the inversion of a large dense matrix to calculate the scattered field. As this task requires $O(N^3)$ calculations where N is the number of grid points, MoM is known to be computationally quite intensive. The fast-multipole technique [2] developed recently can reduce the complexity of MoM-type problems and can be used alternatively as a fast forward solver. Finite-difference techniques are also frequently used as forward solvers and like MoM rely on a full-space discretization. Although the resulting matrices are sparse, one still faces the delicate task of specifying an absorbing boundary condition to terminate the computational grid.

Here we consider the solution of scattering problems using transition matrix (T-matrix) methods [3]–[6]. Unlike finite-difference techniques, the T-matrix approach does not require an absorbing boundary condition and substitutes the discretization of space with harmonic expansions of the fields, thereby reducing the number of unknowns for a wide range of problems. Chew *et al.* have pioneered the development of a number of fast recursive T-matrix algorithms for determining the scattered fields in a variety of scenarios [6]–[12]. These methods basically function by tessellating electrically large objects into small subscatterers whose individual T-matrices can be well represented using low-order harmonic expansions. A recursive formula then is used to aggregate the effects of all the subscatterers to compute the fields.

The motivation for the algorithm in this paper is the desire to solve scattering problems in the near field for the linear array geometry shown in Fig. 1. Specifically, we are interested in the development and verification of a recursive algorithm capable of computing scattered fields from multiple dielectric and/or metallic objects in the near field. For simplicity, we considered an E_z polarized plane wave incident on a two-dimensional (2-D) problem geometry in which multiple scatterers each possessing a circular cross section (i.e., infinite circular cylin-

Manuscript received February 27, 1997; revised November 21, 1997. This work was supported in part by DOE Contract DE-FC07-95ID13395, NSF Grant MIP-9623721, and by Subcontract GC123920NDG from Boston University under the AFOSR MURI Program on Reduced Signature Target Recognition.

The authors are with the Center for Electromagnetics Research, Northeastern University, Boston, MA 02115 USA.

Publisher Item Identifier S 0018-926X(98)03401-2.

ders) are located in an infinite medium of constant complex permittivity. Rather than decomposing each full scatterer into a large number of small subobjects, the goal here is to develop a recursion based on higher order harmonic expansions for the individual large objects. The result is an algorithm comprised of a small number of high-dimensional T-matrix computations rather than a large number of low-dimensional recursions with the idea that the former approach will be more efficient than the latter. For the near-field calculations however, we show that the higher order expansions result in instabilities in the original recursions developed by Chew. By modifying these recursions, we obtain a stable algorithm that avoids these instabilities and is capable of both near and far-field computations. Finally, we demonstrate that this approach retains the low asymptotic computational complexity of the method in [6], but in practice requires far fewer floating point operations.

The remainder of this paper is organized as follows. In Section II we briefly review the recursive T-matrix algorithm for multiple scatterers. In Section III, we discuss how T-matrix techniques can be applied to near-field measurement problems and the modification in the recursive algorithm. In Section IV, we will discuss the results and show examples. Finally, in Section V, we will draw conclusions and suggest future work.

II. Recursive T-Matrix Algorithm

In the recursive T matrix approach of [6] the total scattered field $\psi^{\mathrm{sca}}(\underline{r})$ arising from L scatterers is [6]

$$\psi^{\mathrm{sca}}(\underline{r}) = \sum_{i=1}^{L} \underline{\psi}^{T}(\underline{r_i})\mathbf{T}_{i(L)}\boldsymbol{\beta}_{i,0}\underline{a} \tag{1}$$

with

$$\begin{aligned}\mathbf{T}_{n+1(n+1)}&\boldsymbol{\beta}_{n+1,0} \\ &= \left[\mathbf{I} - \mathbf{T}_{n+1(1)}\sum_{i=1}^{n}\boldsymbol{\alpha}_{n+1,i}\mathbf{T}_{i(n)}\boldsymbol{\beta}_{i,0}\boldsymbol{\alpha}_{0,n+1}\right]^{-1} \\ &\quad\times \mathbf{T}_{n+1(1)}\left[\boldsymbol{\beta}_{n+1,0} + \sum_{i=1}^{n}\boldsymbol{\alpha}_{n+1,i}\mathbf{T}_{i(n)}\boldsymbol{\beta}_{i,0}\right]\end{aligned} \tag{2}$$

and

$$\mathbf{T}_{i(n+1)}\boldsymbol{\beta}_{i,0} = \mathbf{T}_{i(n)}\boldsymbol{\beta}_{i,0} + \mathbf{T}_{i(n)}\boldsymbol{\beta}_{i,0}\boldsymbol{\alpha}_{0,n+1}\mathbf{T}_{n+1(n+1)}\boldsymbol{\beta}_{n+1,0} \tag{3}$$

where $n = 1, 2, \cdots, L$, $i = 1, 2, \cdots, n$, $\mathbf{T}_{i(n)}$ is the T-matrix for the ith object in the presence of n scatterers, $\boldsymbol{\beta}$, and $\boldsymbol{\alpha}$ are translation matrices [4], [5] used to translate T-matrices between different reference coordinate systems denoted by their subscripts (Fig. 1), $\underline{a}$ is a known constant coefficient vector, $\underline{\psi}(\underline{r_i})$ is a column vector comprised of Hankel functions and complex exponentials, and $\underline{r_i}$ is the location vector for the ith scatterer. The recursion starts with the individual T-matrices, $\mathbf{T}_{i(1)}$, of the scatterers.

Theoretically, the matrices $\boldsymbol{\alpha}$, $\boldsymbol{\beta}$, and $\mathbf{T}$ are of infinite dimension. T-matrix algorithms truncate these matrices with finite values N and M such that the residual error is below the machine precision or acceptable levels. Here, N represents the number of harmonics used to expand the fields at the scattering origin O_s (Fig. 1) and M represents the number of harmonics used to expand the fields in the objects' local coordinate systems O_i (Fig. 1), $i = 1, 2, \cdots, L$. The number of harmonics N and M are related to the distances of scatterers from the scattering origin and the radii of the scatterers, respectively. As the distances between scatterers and the scattering origin increase, N needs to be increased and as the radii of scatterers increase, M needs to be increased [6].

III. A Modified Recursive T-Matrix Method

In this paper we desire the scattered field from a collection of spatially separated objects in the near field of a receiver array. While one could tessellate the objects and employ the method of [6] using low-order $(M < 2)$ harmonic expansions, the large number of subscatterers makes such an approach computationally intensive. Rather, we seek an algorithm based on high-order (large M) harmonic expansions for the scattered fields associated with each separate large object. The underlying assumption, shown to be true in Section IV, is that the small number of higher dimensional T-matrix recursions is less costly than a large number of low-order computations. In this section, we show that the use of large M results in an instability in a particular formula upon which the original recursive T-matrix algorithm in (2) and (3) is based, specifically when near-field computations are required. We then present a modified recursion which bypasses this addition formula and results in a stable and efficient method for solving the problem of interest.

A. Determination of Scattering Origin

For the geometries we are interested in this paper, the scattered field is desired in the near or intermediate field. Because of the requirements on the loci of observation points imposed by the harmonic expansion in (1), the scattering origin (x_s, y_s) relative to global origin O_g must be selected such that there must be at least one circle centered at (x_s, y_s), encircling all objects, with no receivers inside it. The dashed circle in Fig. 1 depicts such a circle. Assuming a linear receiver array, the condition to choose the scattering coordinate system is

$$R_c = \max_{i\in\{1,2,\cdots,L\}}\left\{\sqrt{(x_s - x_i)^2 + (y_s - y_i)^2} + a_i\right\} < |y_s| \tag{4}$$

where the triplet $(x_i, y_i; a_i)$ represents x and y coordinates of the center and radius of the ith circular object relative to the global origin O_g. This condition must be met by individual objects as well as by all objects collectively. Therefore, we can rewrite the condition in (4) as the intersection of regions as follows:

$$(x_s, y_s) \in \left\{(x, y)\;\middle|\;\bigcap_{i=1}^{L}\sqrt{(x - x_i)^2 + (y - y_i)^2} < |y| - a_i\right\}. \tag{5}$$

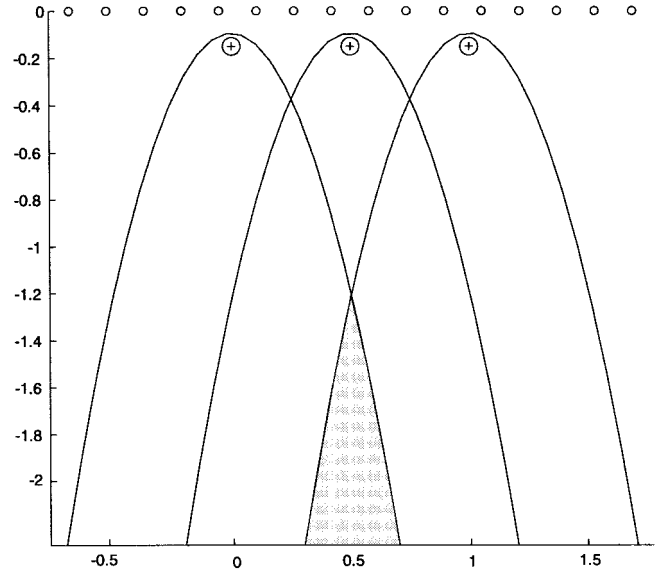

Fig. 2. Scattering origin regions.

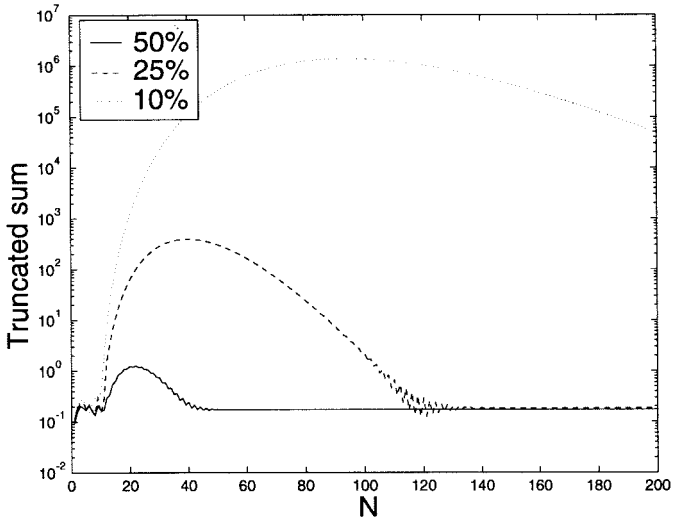

Fig. 3. Convergence pattern of the truncated sum in (7) for $M = 5$. Curves show the convergence for $\underline{\delta} = 0.1\underline{r}_p$, $\underline{\delta} = 0.25\underline{r}_p$, and $\underline{\delta} = 0.5\underline{r}_p$.

In fact, each term under the intersection sign in (5) defines the region under an upside-down parabola. Fig. 2 depicts the parabolic regions for three scatterers in a particular near-field example. Any point inside the shaded area representing the intersection of all three parabolic regions can be selected as the scattering origin. Note that any choice of (x_s, y_s) with $y_s \approx -\infty$ will always satisfy the condition in (4). However, the order of harmonics used in the T-matrix algorithm is proportional to the distance between the scattering origin and object centers [6]. Therefore, the optimum scattering origin should be within this shaded area and as close as possible to the objects to minimize N. As we show in Section III-B, with this choice of (x_s, y_s), the distances between the object centers and the scattering origin can be very close, which causes convergence problems in the addition formulas of T-matrix algorithm for the large M used in our higher order expansions. In Section III-C, we describe a modification in the recursive T-matrix algorithm that lets us use the algorithm with optimum choice of scattering origin.

B. Problems with Higher Order Harmonic Expansions

The convergence problems alluded to earlier can be traced to the fact that (2) uses the identity

$$\boldsymbol{\alpha}_{p,q} = \boldsymbol{\beta}_{p,0}\boldsymbol{\alpha}_{0,q}, \qquad \text{if } |\underline{r}_q| \geq |\underline{r}_p| \tag{6}$$

which, in turn, requires the ordering of the objects such that $|\underline{r}_1| \leq |\underline{r}_2| \leq \cdots \leq |\underline{r}_L|$. By using definitions of $\boldsymbol{\alpha}_{p,q}$, $\boldsymbol{\beta}_{p,0}$, and $\boldsymbol{\alpha}_{0,q}$ [4], [5], we can write the (m, m')th entry $[\boldsymbol{\alpha}_{p,q}]_{m,m'}$ as

$$\begin{aligned} &H^{(2)}_{m-m'}(k|\underline{r}_{pq}|)e^{-j(m-m')\phi_{pq}} \\ &\quad = \lim_{N\to\infty} \sum_{n=-N}^{N} J_{m-n}(k|\underline{r}_p|)e^{-j(m-n)(\phi_p+\pi)} \\ &\qquad \times H^{(2)}_{n-m'}(k|\underline{r}_q|)e^{-j(n-m')\phi_q} \end{aligned} \tag{7}$$

where $\underline{r}_{pq} = |\underline{r}_{pq}|e^{-j\phi_{pq}} = \underline{r}_q - \underline{r}_p$ and $\underline{r}_i = |\underline{r}_i|e^{-j\phi_i}$, $i = p, q$. This truncated sum does not converge if $\underline{r}_q = \underline{r}_p + \underline{\delta}$ where $|\underline{\delta}|$ is small as compared to $|\underline{r}_p|$ and $|\underline{r}_q|$ and if $m - m'$ is a large number ($-M \leq m \leq M$ and $-M \leq m' \leq M$). Fig. 3 shows the convergence of the series in (7) for the corner entries of (6) for $M = 5$, i.e., $\max\{m - m'\} = 10$. Here we have three curves, showing the convergence for $\underline{\delta} = 0.1\underline{r}_p$, $\underline{\delta} = 0.25\underline{r}_p$ and $\underline{\delta} = 0.5\underline{r}_p$. $M \geq 5$ and $\underline{\delta} < 0.1\underline{r}_p$ are typical parameter choices for the problems of interest in this paper. It is clear from this figure that as the magnitudes of the two vectors get closer, the convergence rate slows. Chew *et al.* [10] suggested a windowed addition theorem (which is originally developed for H_z polarized scattering) to overcome this problem, but the implementation of this method introduces two new variables to set the width and shape of the window. In addition, the windowed summation introduces errors in the sum for vectors for which the convergence is not a problem.

It should be noted that not all valid scattering origins for a given problem give rise to this convergence problem. Indeed, trial and error will quickly demonstrate that, for a given collection of scatterers, there exist scattering origins where the original T-matrix recursions work just fine. These points are typically far from the scatterers, thereby requiring large N in the recursions and moreover there does not appear to be an easy means of *a priori* determining whether a chosen origin will or will not give rise to a convergence difficulty. Thus, in the following sections we introduce a modified recursion that bypasses the convergence issue for all valid scattering origins, thereby allowing us to use the closest valid origin (i.e., smallest N) to solve the problem.

C. Modified Recursive T-matrix Algorithm

To eliminate the need for the use of (6), we go one step back in the derivation of recursion formulas and write (2) as

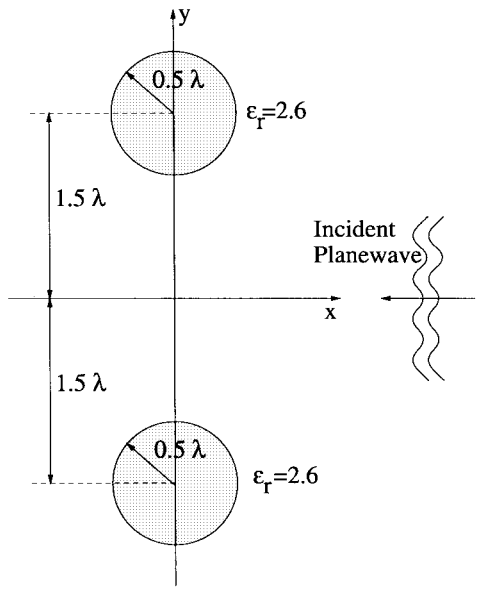

(a)

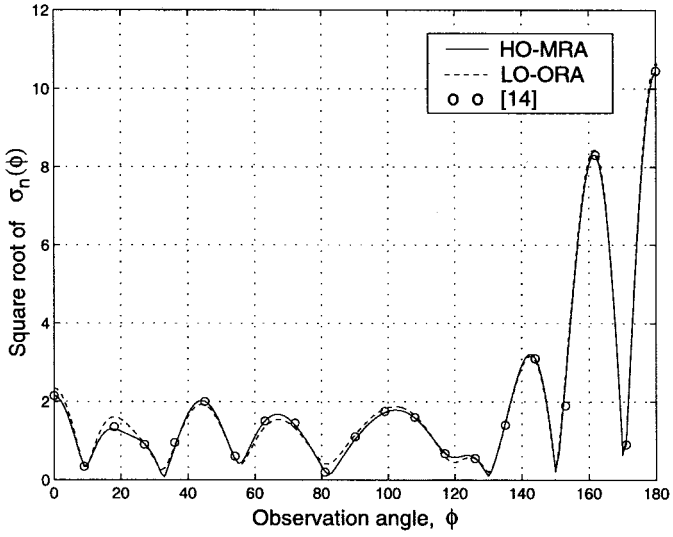

(b)

Fig. 4. Comparison of echo width with [14] for two equal dielectric cylinders. (a) Scattering geometry. (b) Normalized echo width for geometry of (a).

[6, Eqs. (7), (8)]:

$$\mathbf{T}_{n+1(n+1)}\boldsymbol{\beta}_{n+1,0} = \left[\mathbf{I} - \mathbf{T}_{n+1(1)}\sum_{i=1}^{n}\boldsymbol{\alpha}_{n+1,i}\mathbf{T}_{i(n)}\boldsymbol{\alpha}_{i,n+1}\right]^{-1} \times \mathbf{T}_{n+1(1)}\left[\boldsymbol{\beta}_{n+1,0} + \sum_{i=1}^{n}\boldsymbol{\alpha}_{n+1,i}\mathbf{T}_{i(n)}\boldsymbol{\beta}_{i,0}\right] \quad (8)$$

and (3) as

$$\mathbf{T}_{i(n+1)}\boldsymbol{\beta}_{i,0} = \mathbf{T}_{i(n)}[\boldsymbol{\beta}_{i,0} + \boldsymbol{\alpha}_{i,n+1}\mathbf{T}_{n+1(n+1)}\boldsymbol{\beta}_{n+1,0}] \quad (9)$$

without using (6). Since (6) is not used in (8) and (9), we can base a new recursion on these two equations and the identity

$$\boldsymbol{\beta}_{i,0}\boldsymbol{\beta}_{0,i} = \mathbf{I} \quad (10)$$

where $\boldsymbol{\beta}_{i,0}$ is $M \times N$, $\boldsymbol{\beta}_{0,i}$ is $N \times M$, and (10) holds as long as $N > M$, which is always true as long as objects are not overlapping. By using (8)–(10), the modified recursion equations are

$$\mathbf{T}_{n+1(n+1)}\boldsymbol{\beta}_{n+1,0} = \left[\mathbf{I} - \mathbf{T}_{n+1(1)}\sum_{i=1}^{n}\boldsymbol{\alpha}_{n+1,i}\mathbf{T}_{i(n)}\boldsymbol{\beta}_{i,0}\boldsymbol{\beta}_{0,i}\boldsymbol{\alpha}_{i,n+1}\right]^{-1} \times \mathbf{T}_{n+1(1)}\left[\boldsymbol{\beta}_{n+1,0} + \sum_{i=1}^{n}\boldsymbol{\alpha}_{n+1,i}\mathbf{T}_{i(n)}\boldsymbol{\beta}_{i,0}\right] \quad (11)$$

and

$$\mathbf{T}_{i(n+1)}\boldsymbol{\beta}_{i,0} = \mathbf{T}_{i(n)}\boldsymbol{\beta}_{i,0} + \mathbf{T}_{i(n)}\boldsymbol{\beta}_{i,0}\boldsymbol{\beta}_{0,i}\boldsymbol{\alpha}_{i,n+1}\mathbf{T}_{n+1(n+1)}\boldsymbol{\beta}_{n+1,0}. \quad (12)$$

The recursion is still over the same block $\mathbf{T}_{i(n)}\boldsymbol{\beta}_{i,0}$, but since (6) is eliminated, these new recursion equations do not suffer from convergence problems.

It is easily shown that the complexity of modified recursive algorithm is (like that of the original) $O(L^2M^2N)$ with a slightly larger constant in front of M^2N resulting from extra multiplications to obtain $\mathbf{T}_{i(n)}$ from $\mathbf{T}_{i(n)}\boldsymbol{\beta}_{i,0}$. Despite this small increase, we show in the next section that the rise in M associated with the lack of tessellation of the individual large scatterers is more than offset by the corresponding reduction in L—the number of scatterers used in the recursive computation—thereby resulting in large computational savings.

IV. Discussion and Examples

We first verify our new scattering algorithm against published results and then provide a collection of examples that are relevant for near-field applications. As most previously published results for scattering problems involve far-field computations, in verifying our approach we also demonstrate its ability to handle far-zone calculations. Where appropriate, we compare the computational cost of our higher order modified recursive algorithm (HO-MRA) against two alternate T-matrix approaches. First, we implement the lower order original recursive algorithm (LO-ORA) of [6] for near- and far-field problems. For far-zone problems with mixed dielectric and metallic scatterers, we consider high-order (i.e., large M) forms of the original recursions (HO-ORA) (2) and (3), where, because of the far-field assumption, the instability problem is not an issue.

Before we proceed, we define the normalized echo width as [14]

$$\sigma_n(\phi) = \lim_{r\to\infty}\frac{2\pi r}{\lambda}\left|\frac{\psi^{\mathrm{sca}}(\underline{r})}{\psi^{\mathrm{inc}}(\underline{r})}\right|^2 \quad (13)$$

where λ is the wavelength in the medium of propagation.

We first calculated the scattered field due to two dielectric cylinders placed in free space, each with relative dielectric constant of 2.6 and radius of 0.5λ. The distance between the cylinders is 3λ [Fig. 4(a)]. An E_z polarized plane wave

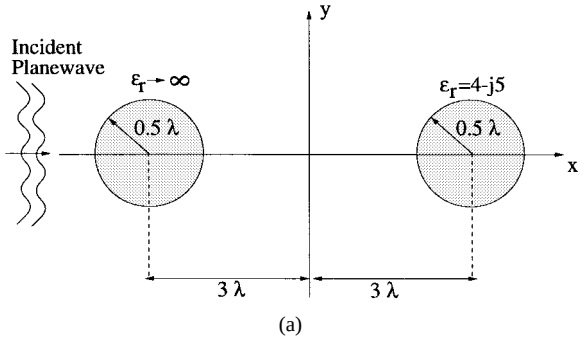

(a)

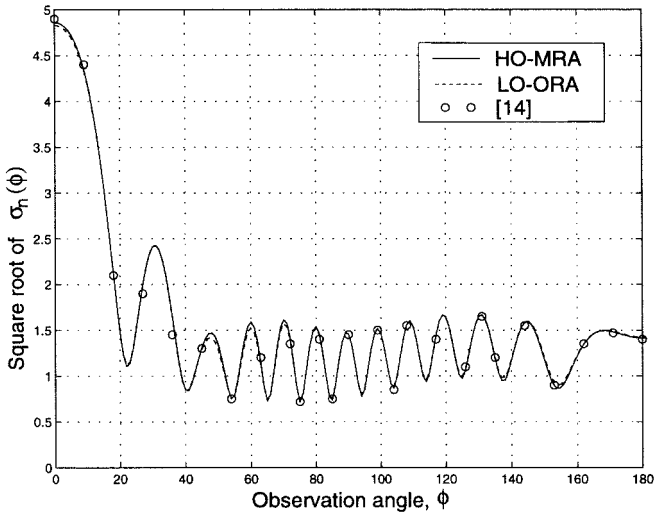

(b)

Fig. 5. Comparison of echo width with [14] for two cylinders, one lossy dielectric, and one metallic. (a) Scattering geometry. (b) Normalized echo width for geometry of (a).

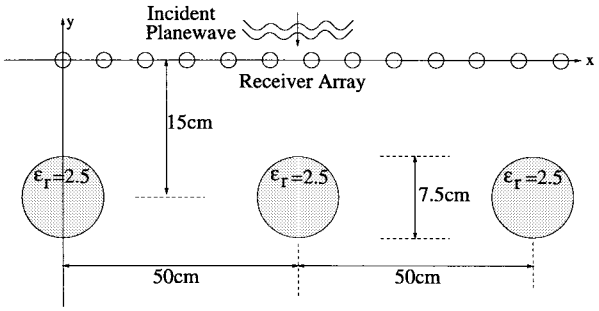

(a)

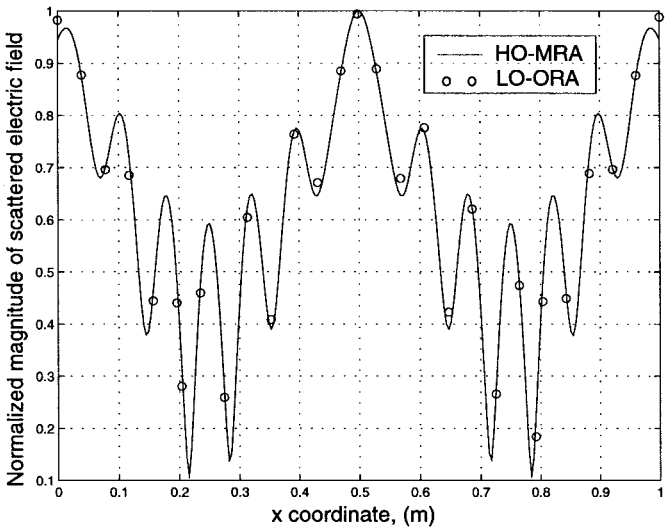

(b)

Fig. 6. Scattered electric field from three dielectric objects. (a) Near-field geometry, all dielectric objects. (b) Scattered field observed along the receivers for geometry of (a).

is incident from 0°. Fig. 4(b) shows the square root of the echo width calculated using the HO-MRA of this paper (solid line), the LO-ORA of [6] (dashed line) and results in [14] (circles). Since HO-ORA produced essentially the same fields as HO-MRA, the results of this approach is not shown here. Fig. 5(b) shows a similar comparison for a mixed object case depicted in Fig. 5(a), i.e., one cylinder is metallic and the other is lossy dielectric with $\epsilon_r = 4–j5$. In this example, to calculate the scattered field using LO-ORA, the conducting scatterers have to be tessellated along their perimeters. In [11] and [12], Gürel *et al.* use metallic strips and patches, whose individual T-matrices are found via MoM, with LO-ORA. Adapting their approach, one can tessellate conducting scatterers with flat or curved metallic strips in the examples. Alternatively, [13] uses small subcylinders along the perimeter of conducting scatterers for tessellation. We have used the second approach with LO-ORA to calculate the scattered field since it does not require the use of MoM. As in the previous example, the square root of the echo width obtained using the modified algorithm, LO-ORA, and that reported in [14] are very close.

Now, we present scattering examples that are representative of near-field applications. All objects are assumed to lie in a homogeneous lossy background ($\epsilon_b = 6\epsilon_0$, $\sigma_b = 5 \times 10^{-2}$ S/m); the operating frequency is 1 GHz and a plane wave is incident from 90° [see Fig. 6(a)]. We first find the scattered field from three dielectric objects with diameters 7.5 cm, as shown in Fig. 6(a). All objects have a relative permittivity of 2.5. The scattering origin has to be placed far away from the receiver array ($x_s = 0.5$ m, $y_s = -1.25$ m), because the objects are close to the receivers, which, in turn, requires a large value (120) for N. For this case, we calculated the scattered field using both the LO-ORA and HO-MRA defined in Sections II and III-C, respectively. Fig. 6(b) shows the normalized scattered fields observed along the receiver array using the HO-MRA (solid line) and the LO-ORA (circles). It is clear from this figure that both approaches yield very similar fields.

The second near-field example depicts a mixed-object case since the objects at the sides are metallic and the object at the center is dielectric with a relative dielectric constant of 2.5 [Fig. 7(a)]. The locations of the objects are the same as the previous example and the scattering origin is still at ($x_s = 0.5$ m, $y_s = -1.25$ m). As a result $N = 120$ and since the object radii are relatively small $M = 12$. The normalized scattered field observed along the receiver array for mixed-object case is shown in Fig. 7(b). As in the far-field example, for LO-ORA implementation, metallic objects are tessellated using the approach in [13].

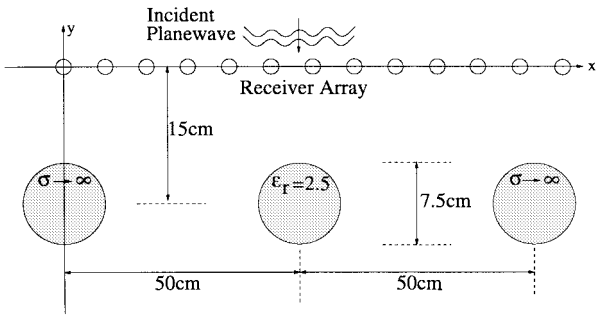

(a)

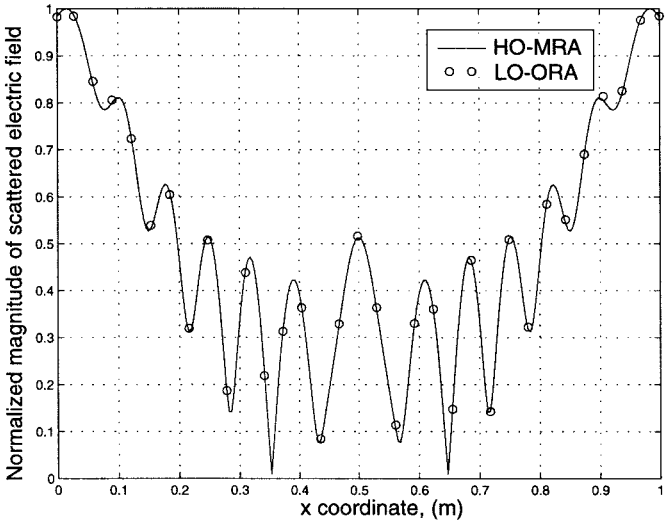

(b)

Fig. 7. Scattered electric field from two metallic and a dielectric objects. (a) Near-field geometry, mixed objects. (b) Scattered field observed along the receivers for geometry of (a).

TABLE I
COST COMPARISON FOR RECURSIVE ALGORITHMS. ALL NUMBERS IN FLOPS/10^6 AND C/P MEANS CONVERGENCE PROBLEMS IN NEAR FIELD CALCULATIONS

	HO-MRA	LO-ORA	HO-ORA
Fig. 4	0.6	1150	0.64
Fig. 5	1.9	766	1.9
Fig. 6	18.94	857	c/p
Fig. 7	18.95	393	c/p

We now compare computational costs of the HO-MRA, LO-ORA, and HO-ORA. To ensure a fair comparison whenever a tessellation is required, we set the density of subscatterers to be close to that used in [6]. Performance of each approach is measured by the floating point operations (flops) required to calculate the scattered field. Table I shows the flop count of all three recursive T-matrix algorithms that can be used to find the scattered fields from multiple, spatially separated cylinders. Table II shows the number of scatterers L, number of harmonics M, N, and the location of the scattering origin (x_s, y_s) used in these examples.

The first two rows of Tables I and II correspond to examples from the 2-D scattering literature. For these cases, all observation points are in the far field so that the convergence problem alluded to earlier is not an issue. As seen from Table I LO-ORA's flop count is quite large as compared to HO-MRA and HO-ORA. The reason behind this large cost is that numerous subscatterers are required for each cylinder. One would expect the computational complexity of HO-ORA to be less than that of HO-MRA since the latter needs extra multiplications to obtain $\mathbf{T}_{i(n)}$ from $\mathbf{T}_{i(n)}\boldsymbol{\beta}_{i,0}$. However, since the scattering origin is placed at a different location in HO-ORA to prevent the convergence problem, the number of harmonics N has to be increased accordingly, which increases the flops required for HO-ORA considerably.

TABLE II
PARAMETER LIST FOR TABLE I

	HO-MRA	LO-ORA	HO-ORA
Fig. 4	L=2,M=7,N=23 (x_s, y_s)=(0,0)	L=398,M=1,N=23 (x_s, y_s)=(0,0)	L=2,M=7,N=28 (x_s, y_s)=(0,0.3λ)
Fig. 5	L=2,M=10,N=40 (x_s, y_s)=(0,0)	L=249,M=1,N=40 (x_s, y_s)=(0,0)	L=2,M=10,N=44 (x_s, y_s)=(0.3λ,0)
Fig. 6	L=3,M=12,N=120 (x_s, y_s)=(0.5,-1.25)	L=93,M=2,N=120 (x_s, y_s)=(0.5,-1.25)	c/p
Fig. 7	L=3,M=12,N=120 (x_s, y_s)=(0.5,-1.25)	L=63,M=2,N=120 (x_s, y_s)=(0.5,-1.25)	c/p

The last two rows of Table I show the flops needed to find the scattered field for near-field examples and Table II shows the number of scatterers, harmonics, and the locus of the scattering origin used in these examples. Unlike previous examples, these geometries require measuring the scattered field in the near field with a linear receiver array, which restricts the regions where the scattering origin can be placed. As we have shown in Section III, the choice of optimum scattering origin results in convergence problems in HO-ORA for near-field geometries. Alternatively, LO-ORA can be used in these problems, however, one has to spend approximately 45 and 21 times more flops than it is needed for HO-MRA for examples in Figs. 6 and 7, respectively.

V. CONCLUSION

In this paper, we present a new recursive T-matrix algorithm specifically designed for the efficient solution of near-field scattering problems involving heterogeneous collections of metallic and dielectric objects. We have verified this algorithm against previously published results, thereby demonstrating its utility for far-field computations and indicated its use for near-field scattering problems. For near- and far-field dielectric scattering problems, this algorithm is significantly more efficient than the subscatterer method in [6]. For far-field computations, the technique in this paper is slightly more costly than the use of higher order expansions in the original recursive formulas.

Even though the forward model in this paper does not take the air–earth interface into account, near-field measurement geometries similar to Figs. 6 and 7 can be used to assess performance of algorithms tailored for processing ground penetrating radar (GPR) data. The forward solver presented in this paper, when used in an inversion scheme, would represent advancement over what is currently used in the literature [15]–[17] in that it solves the near-field multiple scattering problem thoroughly and handles the lossy background.

In terms of genuinely modeling the GPR forward-scattering problem, we are looking to T-matrix-type methods that might allow modeling the air–earth interface relevant in these scenarios without destroying the computational efficiency of the scattering model. Finally, applying the near-field computational abilities of this approach to other application areas would be quite interesting.

ACKNOWLEDGMENT

The authors would like to thank the reviewers for their suggestions, which have significantly improved the clarity of this manuscript.

REFERENCES

[1] R. F. Harrington, *Field Computation by Moment Methods*. New York: IEEE Press, 1993; originally, Malabar, FL: Krieger, 1968.
[2] V. Rokhlin, "Rapid solution of integral equations of scattering theory in two dimensions," *J. Computat. Phys.*, vol. 86, no. 2, pp. 414–439, 1990.
[3] P. C. Waterman, "New formulation of acoustic scattering," *J. Acoust. Soc.*, vol. 45, no. 6, pp. 1417–1429, 1969.
[4] B. Peterson and S. Ström, "Matrix formulation of acoustic scattering from an arbitrary number of scatterers," *J. Acoust. Soc. Amer.*, vol. 56, no. 3, pp. 771–780, Sept. 1974.
[5] W. C. Chew, *Waves and Fields in Inhomogeneous Media*. New York: Van Nostrand Reinhold, 1990.
[6] Y. M. Wang and W. C. Chew, "An efficient algorithm for solution of a scattering problem," *Microwave Opt. Technol. Lett.*, vol. 3, no. 3, pp. 102–106, Mar. 1990.
[7] W. C. Chew, J. A. Friedrich, and R. Geiger, "A multiple scattering solution for effective permittivity of a sphere mixture," *IEEE Trans. Geosci. Remote Sensing*, vol. 28, no. 2, pp. 207–214, Mar. 1990.
[8] W. C. Chew, L. Gürel, Y. M. Wang, G. Otto, R. L. Wagner, and Q. H. Liu, "A generalized recursive algorithm for wave-scattering solutions in two dimensions," *IEEE Trans. Microwave Theory Tech.*, vol. 40, pp. 716–722, Apr. 1992.
[9] W. C. Chew and Y. M. Wang, "A fast algorithm for solution of a scattering problem using a recursive aggregate τ matrix method," *Microwave Opt. Technol. Lett.*, vol. 3, no. 5, pp. 164–169, May 1990.
[10] W. C. Chew, Y. M. Wang, and L. Gürel, "Recursive algorithm for wave-scattering solutions using windowed addition theorem," *J. Electromagn. Waves Applicat.*, vol. 6, no. 11, pp. 1537–1560, 1992.
[11] L. Gürel and W. C. Chew, "A recursive T-matrix algorithm for strips and patches," *Radio Sci.*, vol. 27, pp. 387–401, May/June 1992.
[12] ———, "Scattering solution of three-dimensional array of patches using the recursive T-matrix algorithms," *IEEE Microwave Guided Wave Lett.*, vol. 2, pp. 182–184, May 1992.
[13] A. Şahin and E. L. Miller, "Recursive T-matrix algorithm for multiple metallic cylinders," *Microwave Opt. Technol. Lett.*, vol. 15, no. 6, pp. 360–363, Aug. 1997.
[14] M. Ouda, M. Hussein, and A. Sebak, "Multiple scattering by dielectric cylinders using a multi-filament current model," *J. Electromagn. Waves Applicat.*, vol. 7, no. 2, pp. 215–234, 1993.
[15] J. E. Molyneux and A. Witten, "Diffraction tomographic imaging in a monostatic measurement geometry," *IEEE Trans. Geosci. Remote Sensing*, vol. 31, pp. 507–511, Mar. 1993.
[16] A. J. Witten and J. E. Molyneux, "Ground penetrating radar tomography: Algorithms and case studies," *IEEE Trans. Geosci. Remote Sensing*, vol. 32, pp. 461–467, Mar. 1994.
[17] R. W. Deming and A. J. Devaney, "A filtered backpropagation algorithm for GPR," *J. Environmental Eng. Geophys.*, vol. 0, no. 2, pp. 113–123, Jan. 1996.

Adnan Şahin was born in Kayseri, Turkey, in 1970. He received the B.S. degree from Middle East Technical University, Ankara, Turkey, in 1992, and the M.S. degree from Northeastern University, Boston, MA, in 1994, both in electrical engineering. He is currently working toward the Ph.D. degree in electrical engineering at Northeastern University.

His research interests include computational electromagnetics and the development of efficient signal processing algorithms for inverse scattering problems.

Eric L. Miller (S'90–M'95) received the S.B. degree, in 1990, the S.M. degree, in 1992, and the Ph.D. degree, in 1994 all in electrical engineering and computer science from the Massachusetts Institute of Technology (MIT), Cambridge, MA.

He is currently an Assistant Professor in the Department of Electrical and Computer Engineering at Northeastern University, Boston, MA. His research interests include the exploration of theoretical and practical issues surrounding the use of multiscale and statistical methods for the solution of inverse problems (in general), inverse scattering problems (in particular), and the development of computationally efficient physically based models for use in signal processing applications.

Dr. Miller is a member of Tau Beta Pi, Eta Kappa Nu, and Phi Beta Kappa. He received the CAREER Award from the National Science Foundation in 1996.